ADAPTIVE HUMAN TREMOR ASSESSMENT AND ATTENUATION
Six Degree-of-Freedom Motion Analysis Utilizing Wavelets

Wesley J. E. Teskey, Mohamed Elhabiby and Naser El-Sheimy

Department of Geomatics Engineering, University of Calgary
2500 University Dr. NW, T2N 1N4 Calgary, Alberta, Canada

Keywords: Weighted-frequency Fourier linear combiner (WFLC), Wavelets, Accelerometers, Gyroscopes, Essential tremor, Parkinson's disease, Kalman smoothing, Microelectromechanical systems (MEMS).

Abstract: The use of a weighted-frequency Fourier linear combiner (WFLC) algorithm for assessment and attenuation of movement disorder tremor (including essential tremor and Parkinson's tremor) is quite prevalent; indeed, this technique is likely the most popular for such applications. The novel work presented here applies this technique to accelerometer and gyroscope data describing six degree-of-freedom motion (three translational and three rotational degrees-of-freedom). Most analysis of tremor is based on observation of generally one to three degrees-of-freedom of motion. Six degree-of-freedom motion analysis is more difficult to accomplish because of the complexity of capturing such a large amount of motion data. As well, processing accelerometer and gyroscope data to yield six degree-of-freedom motion generally involves the use of a Kalman smoother (necessary because of signal noise and drift) to ensure that accelerometer signals are correctly compensated for the influence of gravity. After data are processed using a Kalman smoother and the WFLC algorithm is applied, results are interpreted using wavelet frequency spectrum analysis to determine the frequency content before and after processing the data. Results show that the WFLC algorithm can be successfully applied to all six degrees-of-freedom of motion to largely remove tremor.

1 INTRODUCTION

1.1 Movement Disorder Assessment

In recent years there has been much focus on movement disorder tremor assessment using inertial sensors (accelerometers and gyroscopes (Rocon, et al., 2004, 2006)). Such assessment of tremor related disorders (focussing largely on size of tremor, frequency, axis of motion etc.) can help to create a standardized approach to assist medical professionals when diagnosing tremor; this approach can help to better understand the nature of the disorder under evaluation. As well, assessment of tremor can be used to evaluate the effectiveness of medication.

1.2 Movement Disorder Attenuation

Attenuation of tremor is another major focus of recent research conducted. It can take the form of an orthesis designed to actively remove tremor, or passive and active feedback systems to dampen and mitigate tremor (such as a pen with a feedback system such that the tip moves so as to counteract tremor motion). Such attenuation can be quite useful because 90% of tremor patients report a disability (Gallego, et al., 2009).

1.3 Types of Disorders Evaluated

Tremors types evaluated for this research paper include essential tremor (ET) and Parkinson's disease (PD); these are among the most common types of tremor disorders (although, sufferers of these disorders can also exhibit other non-tremor related symptoms) (Rocon, et al., 2004). ET is the more prevalent of these two, affecting 4% of people over age 65 (Louis, 2005); while PD affects 1.5-2.5% of people older than 70 in the United States (Mansur, et al., 2007). Tremor is generally regarded to have a frequency of 3-12 Hz (Elble and Koller, 1990).

2 IMPORTANCE OF KALMAN FILTER

When utilizing accelerometers for tremor assessment and attenuation, it is critical to consider that raw accelerometer data contain both lateral and rotational tremor components (Rocon, et al., 2004). The former tremor type is measured directly by accelerometers and the later is caused by rotation through the gravity field. Indeed, rotating an accelerometer through a gravity field (i.e. about a vector perpendicular to gravity) at a constant rate will cause the accelerometer signal to follow a generally sinusoidal trajectory with peaks at positive gravitational acceleration (generally approximately 9.81 m/s^2 depending on the local gravity field) and troughs at negative gravitational acceleration; this is illustrated in Figure 1. It follows that a rotational tremor (with no lateral motion component) will also register an accelerometer signal depicting tremor motion components. Such a rotational tremor is removed from accelerometer data in this research paper so that the lateral acceleration components can be evaluated independently of rotation. This is shown in Figure 2, an overall flow chart of the data processing. From this figure, it can be seen that processed accelerometer data (bottom half of the figure on the right hand side) is used to evaluate lateral tremor and processed gyroscope data (bottom half of the figure on the left hand side) is used to evaluate rotational tremor.
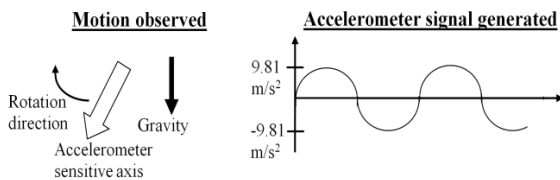
Figure 1: An accelerometer rotated through the gravity field and the signal generated.

To decipher lateral and rotational tremor motion (for six degree-of-freedom motion resolution), a Kalman smoother is employed. Strictly speaking, raw gyroscope data should be sufficient to remove rotational tremor components from accelerometer data by providing orientation information; however, due to signal noise, an accurate solution generally involves extra information and data fusion to accurately obtain orientation data. For the Kalman smoother employed in this research paper, such data fusion uses the known start and end orientation of inertial sensors. As well, updates are performed using accelerometer data during relatively still
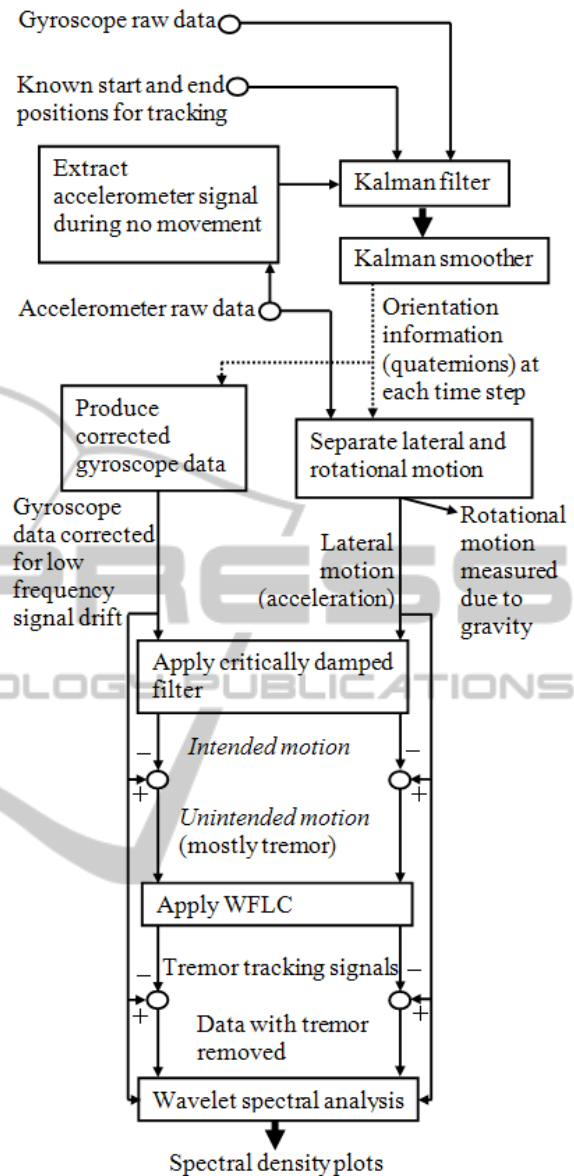
Figure 2: Overall flow chart for data processing.

motion signal portions to estimate orientation about the two horizontal axes (i.e. an orientation reading is performed using an accelerometer *gravity measurement* when the inertial sensors are stationary).

After Kalman smoothing, the weighted-frequency Fourier linear combiner (WFLC) algorithm is used for further analysis. The application of WFLC for the evaluation of all six degrees-of-freedom of tremor motion is novel and is introduced in this research paper likely for the first time. The WFLC algorithm is generally regarded as the most useful for both assessment and attenuation

of tremor (Rocon, et al., 2004).

There are many advantages to using the WFLC technique for six degree-of-freedom tremor analysis. One is that it can allow for medical professionals studying tremor to determine the axis of motion for which tremor is most prevalent for different patients. It also allows for one to determine the degree of correlation of different lateral and rotational tremors and their phase shift with regard to one another. Another feature important for tremor assessment, the overall signal shape (i.e. sinusoidal, zigzag etc.) for each axis of motion, can also be studied.

Six degree-of-freedom motion information is required to properly attenuate tremor for many applications; this is often the case when an external mechanism is used for attenuation (such as implied by the test setup utilized for the research conducted and presented here, where patients were told to simulate eating using a spoon). Such a motion was chosen for analysis because many tremor patients complained about to the fact that they often spilled their soup whilst trying to eat. Studying such a movement is also useful from the perspective of assessment in that significant tremor data is present during evaluation. Future applications stemming from the research carried out could see actuators between the spoon head and handle to mitigate tremor motion.

3 MATHEMATICAL METHODS

3.1 Kalman Filter and Smoother

3.1.1 Kalman Filter

Raw data is first processed to determine sensor orientation for all six inertial sensors used in data collection (three accelerometer and three gyroscopes mounted on a rigid body). The state vector for the Kalman smoother is given as follows:

$$\bar{q} = [q_1, \quad q_2, \quad q_3, \quad q_4]^T \tag{1}$$

Where the first three elements of $\bar{q}$ *indirectly* give rotation magnitude about the x, y and z axes, respectively, and the last element gives the magnitude of overall orientation. The following equations can be used to determine the *Kalman filter a priori* values of the quaternion vector for subsequent time steps under evaluation (as found in (Sabatini, 2006)):

$$\bar{q}_{k+1} = \Phi_{k+1,k}\bar{q}_k \tag{2}$$

and

$$\Phi_{k+1,k} = I_{4,4} + \frac{1}{2}\Omega(\bar{\omega})\Delta t \tag{3}$$

Where Δt is time interval between data readings, $I_{4,4}$ is a four by four element identity matrix and the matrix $\Omega(\bar{\omega})$ is given by:

$$\Omega(\bar{\omega}) = \begin{bmatrix} 0 & -\omega_z & \omega_y & -\omega_x \\ \omega_z & 0 & -\omega_x & -\omega_y \\ -\omega_y & \omega_x & 0 & -\omega_z \\ \omega_x & \omega_y & \omega_z & 0 \end{bmatrix} \tag{4}$$

Elements ω_x, ω_y and ω_z (components of the vector $\bar{\omega}$) are gyroscope measurements for the x, y and z axes respectively. The *Kalman filter a priori* covariance matrix (P) for the quaternion state vector is found for subsequent time steps as follows:

$$P_{k+1} = \Phi_{k+1,k}P_k\Phi_{k+1,k}^T + \Delta t \left(\frac{1}{2}\right)^2 MC_{g,arw}M^T \tag{5}$$

Where

$$M = \begin{bmatrix} -q_4 & q_3 & -q_2 \\ -q_3 & -q_4 & q_1 \\ q_2 & -q_1 & -q_4 \\ q_1 & q_2 & q_3 \end{bmatrix} \tag{6}$$

And $C_{g,arw}$ is a three by three covariance matrix for gyroscope measurements populated with non-zero elements along only the main diagonal as in Sabatini (2006). Values for the matrix are found using an angular random walk formulation as in El-Sheimy, et al. (2008), Shin (2005) and Stockwell (2010).

A standard *Kalman filter a posteriori* update procedure is used as in Chui and Chen (1991) and Grewal (1993). Updates are taken from known start and end orientations of the inertial sensors and accelerometer data measurements during periods of *relatively* stationary or limited motion (stationary or limited motion is determined from when accelerometer signals show low standard deviation and have a combined signal strength roughly equivalent to gravity). Such accelerometer *gravity measurements* can provide orientation information for two of the three axes of orientation (the two lying in the horizontal plane).

3.1.2 Kalman Smoother

After Kalman filtering has finished, a Rauch-Tung-Striebel (RTS) Kalman smoother is applied as given in Brown and Hwang (1992) and Shin (2005). This

smoother has the effect of removing discontinuities in the processed data and improving data quality.

Once orientation data has been found and smoothed, it can be used to correct accelerometer signals for gravitational measurements. This is done by using a rotation matrix at each time step ($\hat{R}$) to transform accelerometer data ($\bar{a}$) (which lie in the *coordinate frame of the moving IMU (Inertial Measurement Unit)*) into a *consistent coordinate frame*. Such a *consistent coordinate frame* is fixed relative to the earth so that gravity ($\bar{g}$) can be subtracted from the signal. After gravity is removed, the remaining accelerometer data are transferred back into the *IMU coordinate frame*, as follows:

$$\bar{a}_t = \hat{R}^{-1}(\hat{R}\bar{a} - \bar{g}) \qquad (7)$$

Where superscript -1 denotes matrix inversion and $\bar{a}_t$ is accelerometer data with only translational motion components remaining (and not influenced by gravitational acceleration). $\hat{R}$ can be found directly from Kalman smoothed quaternion values ($\hat{q}$), as depicted in Altmann (1986) and Kuipers (1999)). As well, $\bar{g}$ (a three element vector) will have values of 0, 0 and $-g_m$, respectively, for its x, y and z axes (where g_m is the magnitude of gravitational acceleration) if the *consistent coordinate frame* chosen is that of the IMU start position as depicted in Figure 4 (a).

3.2 Application of the WFLC Algorithm

3.2.1 Critically Dampened Filter

Processed gyroscope data (raw data with low frequency error drifts removed) and processed accelerometer data (with the gravitational influence on signals removed) are evaluated using a critically dampened filter. This filter was found to be the best in estimating *intended motion* (i.e. motion with tremor components removed) when compared to a number of popular alternatives based on its ability to adequately track a signal without being influenced by signal components with significant tremor (Gallego, et al., 2009). The filter effectively uses a least squares straight line fit of data with more recent data being given a higher weight (i.e. more influence on the fitting line parameters) than previous data (Brookner, 1998).

3.2.2 WFLC Algorithm

The WFLC algorithm fits a series of sinusoidal signals (harmonic sines and cosines referenced to a fundamental frequency) to the data under evaluation (Riviere, et al., 1997). In its early development, it was used for removing the tremor of a surgeon's hand during critical operations by using a feedback system and electric actuators within a surgical instrument to counteract tremor (Riviere, et al., 1998). The algorithm also is quite useful for describing and removing movement disorder tremor because of its ease of implementation (i.e. simplistic mathematical iterations are utilized), zero phase lag real time filtering capabilities and its relative computational efficiency (utilizing just a small number of iterative computational steps).

3.3 Wavelet Spectral Analysis

Pre and post WFLC processed inertial data (both with gravitational effects on accelerometer data removed) are analyzed using wavelets to determine the frequency spectrum. The main advantages of using wavelets for such an application is the localization power in both frequency and time domain (so non tremor signal portions between trials can be easily negated) and the availability of numerous base functions, that can be used as mother wavelet function, leading to better signal modelling; as opposed to Fourier based analysis which is largely focussed on the use of sinusoidal functions for analysis.

A continuous wavelet transform was used to allow for a more thorough visual inspection of the signal evaluated than can be afforded using a discrete wavelet transform. The continuous wavelet transform is found as follows (Goswami and Chan, 1999):

$$w(p_j, t_k) = \frac{1}{\sqrt{p_j}} \int_{-\infty}^{\infty} s(t)\tilde{\psi}(\frac{t-t_k}{p_j})dt \qquad (8)$$

Where p_j is a scaling coefficient to allow for analysis of different frequencies of interest, t_k is a time shift parameter that allows for localization of the analysis, $s(t)$ is the inertial signal under evaluation at time t and $\tilde{\psi}$ is the mother wavelet analyzing function's complex conjugate. Wavelet scales selected (given as j in (8)) for evaluation span 1 to 64 (with corresponding *pseudo-frequencies* of 91.8 Hz and 1.4 Hz respectively; these *pseudo-frequencies* are found by scaling the wavelet center frequency (Matlab, 2008)). Such a broad frequency spectrum for analysis allows for an in depth view of the signal under examination.

A coiflets wavelet of order three was used for evaluation because it matched closely with the data when compared to other possible wavelet candidate

functions. The coiflets 3 mother wavelet is shown in Figure 3.

4 EXPERIMETNAL METHODS AND RESULTS

4.1 Data Collection

Figure 4 depicts the manner in which data was collected from test subjects (note the IMU axes labels in Figure 4 (a)). Test subjects lifted an IMU out of a holster and simulated eating using a spoon attached to the IMU (simulating only one placement of food into their mouth). Upon completion of this task, the returned the IMU to the holster; ten such tests were carried out for each subject under evaluation. In this manner, both the start and end orientation of the IMU were known (relative to one another) which is important for implementation of the Kalman filter and smoother depicted in sub-section 3.1.
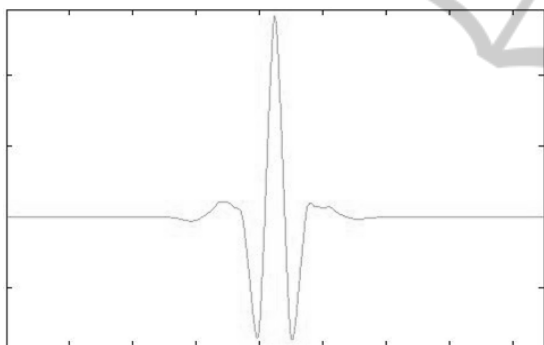
Figure 3: The coiflets 3 mother wavelet.

Data logging took place at 130 Hz. The IMU used was manufactured by the Mobile Multi-Sensor Systems (MMSS) research group at the University of Calgary. A tri-axial accelerometer (LIS3L06AL from ST Microelectronics (2006)) and three single-axis gyroscopes (XV-8100CV from Epson Toyocom (2010)) were utilized.

During experimentation, 11 controls (7 female), 9 ET patients (3 female) and 30 PD patients (20 female) were evaluated using testing that had received ethics approval from the Conjoint Health Research Ethics Board at The University of Calgary. The mean age of controls was 64.1, for ET patients it was 64.8 and for PD patients it was 66. A number of patients (2 ET and 27 PD) were on medication to help reduce tremor. For the ET patients, this medication was largely ineffective (based on conversation with the patients and results of the data analysis presented here) and for PD patients it had varying effectiveness depending on when they last took their medication and how large the dosage was.

Patients with the most significant tremor (8 of the ET patients and 9 PD patients) were evaluated separately for the analysis in the following sections of this research paper. These patients were selected based on a thresholding criteria that required their tremor to be one standard deviation in excess of the tremor measured for controls (for at least one of the six inertial signals evaluated), based on the mean absolute value of wavelet details coefficients at scale 18 (corresponding to approximately 5.1 Hz). A higher value for details coefficients suggested more tremor motion was present. Test subjects that did not pass this thresholding criteria produced data that largely resembled that of controls and therefore such data is not displayed in the following sections of this research paper.

Figure 4 (a): A test subject prior to evaluation.

Figure 4 (b): A test subject during evaluation.

4.2 Kalman Smoothing and WFLC

The Kalman smoothing algorithm was very effective in removing gravitational readings from accelerometer signals. A representative example of this is shown in Figure 5 for a control.

It is important to note that the raw data signal in Figure 5 has extended periods of time in which it is continuously a long distance from the zero acceleration mark. This is expected because gravitational readings can influence the sensors, depending on their orientation. When gravity's impact is removed, the signal remaining only has short durations when it is not near the zero accelerometer reading. This illustrates the value of using the algorithm outlined because the remaining accelerometer data, for the most part, only have lateral motion information embedded within them, making subsequent data analysis significantly more useful than if raw data were used.
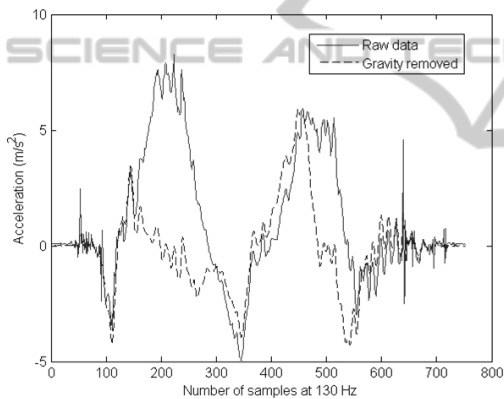
Figure 5: An x-accelerometer signal before and after Kalman smoothing to remove gravitational readings.

After accelerometer signals are corrected as depicted in Figure 5, they are analysed (along with processed gyroscope data) using a critically dampened filter. The goal is to estimate the *intended motion* of the test subjects under evaluation. The results for this are shown in Figure 6 for an ET subject. Generally, the critically dampened filter performed quite well and was a very efficient filter for estimating *intended motion* of test subjects. One issue that if unavoidable with such a filter is that if the influence of past measurements if kept high (in the least squares sense), the filter will lag the signal under evaluation; however, if the influence of past measurements is reduced, then the filter does not remove all tremor motion components. A balance needs to be struck to ensure both adequate tracking and tremor removal are achieved. The results given

in Figure 6 are generally representative of results for all inertial data when a subject with high tremor is evaluated. In this case, a small amount of residual tremor remains in the processed signal; but the ability of the critically damped filter to track the signal adequately, so as to approximate *intended motion*, is reasonable.

After the critically damped *intended motion* approximation is removed from the signal, the remaining signal portion can be evaluated using the WFLC algorithm. Application of this algorithm required a two stage iteration at each time step, the first iteration was used to find the fundamental frequency of the tracked signal and the second iteration was used to find the numerical weights for sinusoids tracking the signal. Multiple iterations were sometimes required at the same time step to allow the algorithm to sufficiently converge to a solution (particularly with the gyroscope data which had a large dynamic range). A representative sample for the WFLC motion approximation is shown in Figure 7; it is a close up of a signal portion of the data displayed in Figure 6.
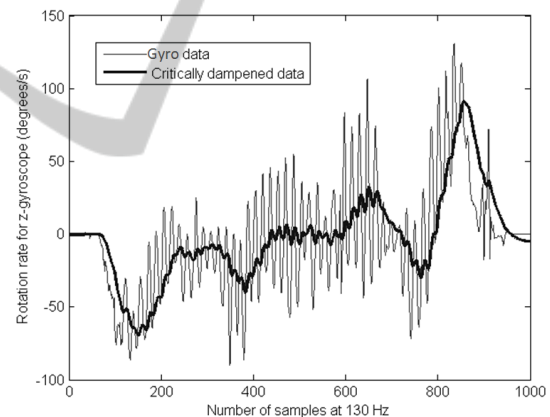
Figure 6: A processed z-gyroscope signal before and after a critically damped filter is applied to approximate *intended rotational motion*.

It is clear from Figure 7 that the WFLC algorithm tracks tremor quite well. The result depicted is quite typical for all inertial data evaluated. Given such an approximation of the tremor, it is possible to very precisely pinpoint the frequency of the tremor observed and its magnitude. This is useful for assessment because it allows for medical professional to evaluate how tremor varies between patients and for the same patient before and after medication is taken.
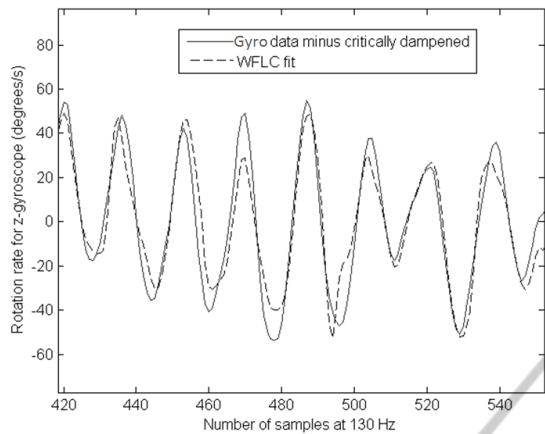
Figure 7: A processed z-gyroscope signal portion and its WFLC approximation depicting rotational motion.

For the purposes of attenuation, the WFLC algorithm provides the signal to be removed from motion to mitigate tremor. The WFLC algorithm is especially useful for attenuation because its zero phase lag property allows for accurate and real time tremor suppression which is critical for many attenuation applications.

4.3 Wavelet Spectral Analysis

Signals can be compared before and after removal of WFLC tremor components to evaluate their frequency spectrum. Such an analysis can assist one in understanding what components of motion have been removed and whether tremor frequencies of interest have been adequately targeted (3-12 Hz). It also helps one to understand how useful the WFLC algorithm is for assessment by depicting how well the tremor motion can be tracked.

In Figure 8, the results of applying the continuous wavelet transform to the signal in Figure 6 (with the critically dampened portion of motion removed) are shown; lighter colours depict that more frequency content is present.

When comparing Figure 8 to Figure 6, it is clear that when a great deal of tremor motion is present, the amount of signal energy depicted in the 3-12 Hz frequency band increases significantly. Thus, Figure 8 validates the use of a coiflets 3 wavelet for the application undertaken (given that other inertial signals processed gave similar results).
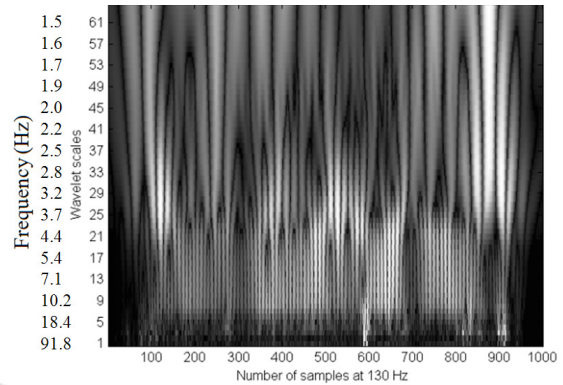
Figure 8: Wavelet processed z-gyroscope data (only *unintended tremor motion* is processed for rotational movement).

The overall (population) results for the data analyzed are given in Figures 9 and 10 for a representative accelerometer axis of motion and gyroscope axis of motion, respectively. Tellingly, the results for all three accelerometer axes of motion were very similar as were the results for all three gyroscope axes of motion. This tends to indicate that tremor acts along all axes of motion concurrently and also that it can be removed in a similar fashion (using the critically dampened and WFLC algorithms) for all of these axes. The results depicted were found by taking the mean magnitude of details coefficients at each wavelet scale for all test subjects of a particular group.
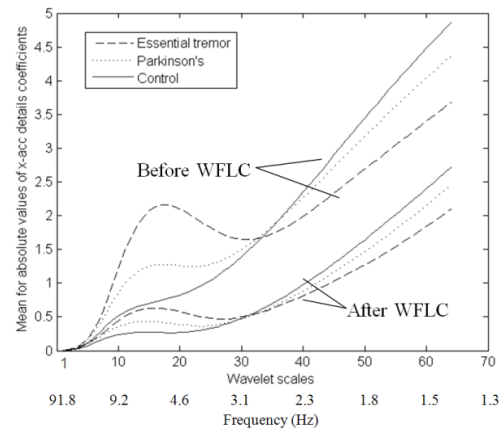
Figure 9: x-accelerometer wavelet spectral analysis for lateral tremor

It can be seen from the results in Figures 9 and 10 that the frequency of the tremor measured for both ET and PD patients was within the expected 3-12 Hz range (as depicted by a bulge in the data displayed within this band). ET patients generally

depicted more tremor that PD patients, which corresponds well to the fact that most ET patients were not on medications for treatment while most PD patient were.

Tremor was reduced substantially for all three groups examined (ET, PD and control) when the WFLC algorithm was applied and it decreased in a proportionate manner, such that those with more tremor before processing also had more frequency content remaining in their motion after application the WLFC algorithm. Signal noise was also likely reduced inadvertently. One of the more significant results is that in the 3-12 Hz range, all three groups evaluated with the WFLC technique had less tremor after evaluation than the control group had before evaluation.

One unfortunate drawback of the analysis is that it seems to remove a lot of low and high frequency motion (as is evident in Figures 9 and 10) along with the 3-12 Hz frequency band of interest.

The high frequency motion likely represents jerky motion, such as when a subject inadvertently struck the IMU on the table during testing. Likely, for mechanical attenuation applications, some kind of thresholding criteria will need to be applied to ensure such signal spikes are not processed, because mitigation of such motion is likely unrealistic due to limits in the operation range of mechanical equipment.
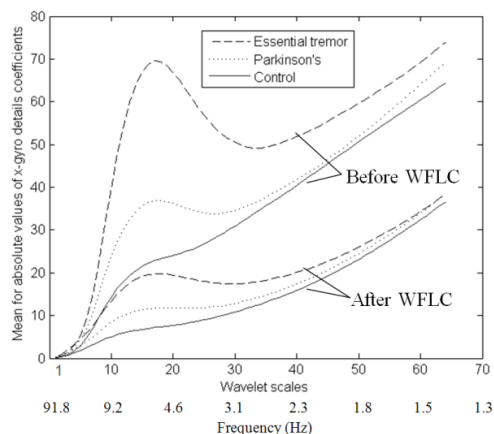
Figure 10: x-gyroscope wavelet spectral analysis for rotational tremor.

The low frequency motion removed likely represents the inadequacy of the critically dampened filter in tracking *intended motion*. Determining which motion is *desired* and which is not is a very difficult research challenge that has been studied for many years (Rocon, et al., 2004). Clearly, there still remains some work to be done to find and appropriate algorithm that is adequately computationally fast and has zero phase lag.

5 SUMMARY AND CONCLUSIONS

The analysis performed validated the use of the Kalman smoothing scheme depicted for removal of the gravitational influence on accelerometer signals. This was necessary so that accelerometer data would properly depict the lateral motion under consideration.

The most significant finding of this research paper is that a combination of a critically dampened filter and the WFLC technique adequately removed the tremor components of motion within the 3-12 Hz frequency band; this was likely applied for the first time in six degrees-of-freedom for movement disorders in this research paper. The same procedure was applied to all motion axes with quality results in all cases.

Another significant finding of this research paper is that the wavelet analysis performed was well suited for the evaluation of a frequency spectrum. The coiflets 3 wavelets was quite capable of realizing tremor motion components, and provided a useful tool for identifying motion at frequencies of interest.

ACKNOWLEDGEMENTS

REFERENCES

Altmann, S. L., 1986. Rotations, Quaternions and Double Group. *Dover Publications*.

Brookner, E., 1998. Tracking and Kalman filtering made easy. *John Wiley & Sons, Ltd*.

Brown, R. G., Hwang, P. Y. C., 1992. Introduction to Random Signals and Applied Kalman Filtering. *John Wiley and Sons Inc. 2nd edition*.

Chui, C. K., Chen, G., 1991. Kalman Filtering With Real Time Applications. Springer-Verlag. 2nd edition.

Elble R J, Koller W C. Tremor. Baltimore: The John Hopkins University Press; 1990.

El-Sheimy, N., Hou, H., Niu, X, 2008. Analysis and modeling of inertial sensors using Allan variance. *IEEE Transactions on Instrumentation and Measurement*, 57(1), pp. 140-149.

Gallego, J. A., Rocon, E., Roa, J. O., Moreno, J. C., Koutsou, A. D., Pons, J. L., 2009. On the use of inertial measurement units for real-time quantification of pathological tremor amplitude and frequency. In *Proceedings of the Eurosensors XXIII conference. Procedia Chemistry 1*, pp. 1219–1222.

Goswami, J. C., Chan, A. K., 1999. Fundamentals of Wavelets: Theory, Algorithms and Applications. Wiley Series in Microwave and Optical Engineering, Wiley-Interscience.

Grewal, M. S., 1993. Kalmen Filtering: Theory and Practice. Prentice-Hall.

Kuipers, B. J., 1999. Quaternions and Rotation Sequences: A Primer With Applications to Orbits, Aerospace and Virtual Reality. *Princeton University Press*.

LIS3L06AL MEMS Inertial Sensor Data Sheet, 2006. ST Microelectronics, pp. 1-17, [Online]. Available: http://www.st.com/stonline/products/literature/ds/11669.pdf [Accessed 13 July, 2010].

Louis, E. D., 2005. Essential tremor. Lancet Neurol, 4, pp. 100-110.

Mansur, P. H. G., Cury, L. K. P., Andrade, A. O., Pereira, A. A., Miotto, G. A. A., Soares, A. B., Naves, E. L. M., 2007. A Review on Techniques for Tremor Recording and Quantification. Critical Reviews in Biomedical Engineering, 35(5), pp. 343-362.

Matlab (computational environment) Help Documentation, 2008. scal2frq function, [Online]. Available:http://matlab.izmiran.ru/help/toolbox/wavelet/scal2frq.html [Accessed 13 July, 2010].

Riviere, C. N., Rader, R. S., Thakor, N. V., 1998. Adaptive Canceling of Physiological Tremor for Improved Precision in Microsurgery. *IEEE Transactions on Biomedical Engineering*, 45(7), pp. 839-846.

Riviere, C. N., Reich, S. G., Thakor, N. V., 1997. Adaptive Fourier Modeling for Quantification of Tremor. Journal of Neuroscience Methods, 74, pp. 77-87.

Rocon, E., Belda-Louis, J. M., Sanchez-Lacuesta, J. J., Pons, J. L., 2004. Pathological Tremor Management: Monitoring, Compensatory Technology and Evaluation. Technology and Disability, 16, pp. 3-18.

Rocon de Lima, E., Andrade, A. O., Pons, J. L., Kyberd, P., Nasuto, S. J., 2006. Empirical Mode Decomposition: a Novel Technique for the Study of Tremor Time Series. Med Bio Eng Comput, 44, pp. 569- 582.

Sabatini, A. M., 2006. Quaternion-based extended Kalman filter for determining orientation by inertial and magnetic sensing. *IEEE Transactions on Biomedical Engineering*, 53(7), pp. 1346-1356.

Shin, E., 2005. Estimation Techniques for Low Cost Inertial Navigation. Ph.D. Department of Geomatics Engineering, University of Calgary.

Stockwell, W., Angle Random Walk. Crossbow Technologies Inc., pp. 1-4, [Online]. Available: http://www.xbow.com/pdf/AngleRandomWalkAppNote.pdf [Accessed 13 July, 2010].

XV-8100CB ultra miniature size gyro sensor data sheet. Epson Toyocom, pp. 1-2, [Online]. Available: http://www.frank-schulte.com/media/Pdf/XV-8100CB_E06X.pdf [Accessed 13 July, 2010].